Mausset-Bonnefont *et al.*
Arthritis Research & Therapy (2025) 27:42
https://doi.org/10.1186/s13075-025-03507-w

Arthritis Research & Therapy

RESEARCH

Open Access

Longitudinal assessment of structural and locomotor deficits as a prediction of severity in the collagenase-induced mouse model of osteoarthritis

Anne-Laure Mausset-Bonnefont[1†], Karine Toupet[1†], Christian Jorgensen[1,2] and Danièle Noël[1,2*]

Abstract

Background The aim of this study was to provide an in-depth longitudinal locomotor and structural characterisation of the collagenase-induced osteoarthritis (CIOA) mouse model, using the most relevant and up-to-date non-invasive locomotor phenotyping and imaging methods. The ultimate goal of this study was to predict histological scores, the gold standard parameter in osteoarthritis (OA), based on locomotor or structural deficits.

Methods The CIOA model was induced in C57BL/6 male mice, which were then maintained in their home cage with or without a running wheel for 6 weeks. Both global and fine locomotor effects were measured using the open field and Catwalk™ tests. Imaging of bone and cartilage was performed using either µCT, contrast-enhanced µCT or confocal laser scanning microscopy (CLSM) at different time points. Correlations between functional or structural changes and histological scores were sought in order to provide tools for predicting histological degradation.

Results Locomotor deficits were observed at early time points (days 3 to 9) but did not persist to the end of the experiment. Signs of inflammation appeared as early as day 9. They worsened on day 28 as the disease progressed and meniscal calcifications were observed by µCT. The early functional and structural changes correlated with the histological scores measured post mortem and some specific locomotor or structural parameters were identified as predictors of histological changes. Free exercise (voluntary running wheel activity) did not seem to influence the severity of the observed changes.

Conclusions Open-field quantification of kinetic parameters is a simple and timely relevant test to detect early locomotor changes and predict histological changes. Meniscal calcifications and osteophyte formation, which can be observed by µCT at early time points, are also highly predictive of OA severity. These two non-invasive techniques are very useful for longitudinal monitoring of mice and OA score prediction.

Keywords Osteoarthritis, CIOA mouse model, µCT, Cartilage imaging, Locomotor evaluation

†Anne-Laure Mausset-Bonnefont and Karine Toupet equally contributing co-authors.

*Correspondence:
Danièle Noël
daniele.noel@inserm.fr
Full list of author information is available at the end of the article

Introduction

Osteoarthritis (OA) is the most common joint disease affecting more than 240 million people worldwide [1]. The disease is characterized by cartilage degradation, low-grade chronic synovial inflammation and bone changes, including subchondral bone sclerosis and periarticular osteophyte formation, leading to pain and functional disability. Several mouse models of OA have been developed to study the pathophysiology and therapy of OA. Surgical and chemically-induced models designed to mimic post-traumatic and inflammatory OA are the most common [2]. Among these models, the collagenase-induced osteoarthritis murine model (CIOA) is characterized by synovial membrane inflammation following collagenase-induced joint instability, which leads to pain, particularly in the early stages, and promotes cartilage destruction and bone sclerosis in the longer term [3].

The gold standard for analysing OA is conventional histopathology scoring, which directly visualizes changes in bone and cartilage in the mouse knee. Magnetic resonance imaging (MRI) can assess soft tissues within the joint, including ligaments, synovium, menisci and cartilage and can provide information about bone architecture. Its non-invasiveness allows longitudinal analysis, but spatial resolution remains low in mouse models, even when relying on µMRI. [4]. On the contrary, detailed 3D imaging of joints by microcomputed tomography (µCT) is also increasingly used as a non-invasive and highly sensitive technique due to its excellent spatial resolution combined with 3D capability [5]. It is used to quantitatively investigate bone structural parameters in different bone compartments [6]. Despite its excellent resolution for imaging mineralized tissue, µCT has poor contrast for soft tissue visualization due to its radiolucency [6]. This limitation can be overcome by the use of radiopaque stains like phosphotungstic acid (PTA), which preferentially reveals collagenous structures and is an excellent contrast agent for imaging cartilage by contrast-enhanced µCT [7]. However, 3D microstructural and topographic imaging of articular cartilage is better elucidated by confocal laser scanning microscopy (CLSM), which has the advantage of providing microscopic resolution [8]. Nevertheless, with the exception of µCT, which can be used for longitudinal analysis of the bone, these techniques are destructive and can only be performed after euthanasia.

In addition to imaging techniques, functional analyses are increasingly being used to predict the course of OA and to monitor the effect of treatments in various animal models using non-invasive methods. Tests to assess thermal hyperalgesia, such as Hargreaves' method, hot plate and tail flick tests, are rarely used because of the risk of injury (minor burns and pain). Mechanical allodynia can be assessed by applying an increasing force to a hind paw using the von Frey test. Static weight bearing, evaluated using an incapacitance meter, is used to compare the weight bearing capacity of the hind paws and has been shown to be reliable in several rodent models of OA [9]. Motor coordination, assessed by rotarod analysis, is measured by calculating the time that animals can remain on a rotating rod but has shown poor reliability in assessing pain in rodent models of OA [10]. The open field test, which analyses the locomotor, exploratory and anxiety-like behaviour activity of mice in an open square arena (45×45 cm), has demonstrated reduced total distance travelled, walking time and rearing time, in mice with age-related OA [11]. Gait analysis monitors the natural gait of mice, including natural speed and paw print analysis on free-walking systems. The relevance of such a technique has been evaluated in a surgically induced mouse model of OA [12]. Potential biases may be associated with some functional tests and it is still unclear which tests are most sensitive, specific and consistent for each model [9]. Moreover, a single functional test is unlikely to be able to detect all behavioural changes associated with OA, which may vary between different animal models.

In the CIOA model, we have previously reported on the interest of combining µCT and CLSM analyses to quantify the effects of different treatments [13–15]. However, little behavioural data are available in this model to date. The aim of this study was to provide a multimodal analysis combining the most relevant locomotor and imaging assessments in the CIOA mouse model and to correlate functional parameters with structural changes at the joint level. In addition, the impact of free exercise, as provided by free access to a running wheel, has been evaluated. The ultimate goal of the study was to provide recommendations for assessing the development of OA and for predicting histological deficits based on structural or functional deficits.

Materials and methods

Collagenase-induced osteoarthritis model

Animal procedures were performed in an animal facility certified by the French health authorities (agreement D34-172–36) and in accordance with the European guidelines (Directive 2010/63/EU). They were approved by the Languedoc-Roussillon Animal Research Ethics Committee (CEEA-LR n°36) and the French Ministry of Higher Education and Research (approval APAFIS#5349–2016050918198875). The work has been reported in line with the ARRIVE guidelines 2.0. In vivo experiments were performed on 10 week-old male C57BL/6 mice obtained from the Janvier laboratories (St. Berthevin, France) and maintained in a specific-pathogen-free animal facility with 12:12 light/dark cycle,

and food and water ad libitum. The CIOA model was induced by two injections of 1 U type VII collagenase (Sigma-Aldrich) in 5 µL saline into the intra-articular space of the right hind knee joint of mice using a 10 µL syringe (Hamilton) with a 25 gauge needle, on days 0 and 2 (OA group). Control mice received 5 µL of saline into the intra-articular space of the right hind joint on days 0 and 2 (Ctrl group). To study the effect of exercise on the development of OA, all the mice, except one group that was euthanized on day 42, were housed in cages containing a 12 cm diameter running wheel devoid of the capacity to automatically measure any distance or duration parameters. Mice were allowed to run freely on the running wheel.

Functional tests

Functional tests (open field and Catwalk™ gait analysis) were performed one day (D-1) before the first collagenase injection and then at D3, D7, D9, D13, D29 and D42 for open field and at D3, D9 and D29 for Catwalk™ (we focused on these 3 time points for Catwalk™ because previous pilot experiments never showed any changes at D13 compared to D9 and D42 compared to D29).

Global locomotion was assessed by the open field test (Infrared Actimeter, Bioseb, France): each animal was placed in the center of the arena and its behaviour was recorded with infrared beams for 10 min. Several parameters were measured: distance covered, speed, rest time and time spent in fast movements (i.e. over 5 cm/s).

Gait was analysed using the Catwalk™ system (Noldus Information Technology, the Netherlands) in a dark room, with the exception of the computer screen light. Mice were allowed to voluntarily cross a 100 cm long, 5 cm wide catwalk with a glass platform illuminated by green fluorescent light. When a mouse's paw touches the glass floor, the green light entering through the long edge of the glass is scattered, creating an illuminated image in which the intensity of the light correlates with the force exerted by the paw. Footprints captured by a high-speed camera placed under the glass floor were analysed using the Catwalk™ XT 10.1 software. Mice were allowed to spontaneously cross the catwalk as many times as necessary to obtain three compliant runs, defined as runs with at least three consecutive complete step cycles of all four paws without stopping, hesitating, running or bounding. For the analysis, each video was meticulously examined and reconstructed for each run in detail. Each run was considered compliant if there was no missing paw or asynchronous gait. In the event that this was the case, the run was to be excluded from the analysis. Data are reported as the average of the three runs per mouse. We analysed several parameters, including stand time (i.e. duration of paw contact with the glass plate, expressed in seconds), swing (i.e. duration of no paw contact with the glass plate, expressed in seconds), print area (i.e. surface area of the entire footprint, expressed in cm^2), base of the hind paws (i.e. width between the hind paws, expressed in mm), and duty cycle (i.e. proportional duration of a paw placement on the ground during a step cycle (stance + swing), expressed as a percentage).

Analysis of bone parameters

Mice were euthanised either on day 9 (D9) and day 28 (D28) (7 mice/group) or on day 42 (D42) (10 mice/group). Injected and contralateral hind paws were collected and fixed in 4% formaldehyde for further analysis. After fixation, the hind paws were scanned using a micro-computed tomography system (µCT SkyScan 1176, Bruker). Each scan was performed with the following parameters: 0.5 mm aluminium filter, 50 kV, 500 µA, 18 µm pixel size and 0.5° rotation angle. The images were then reconstructed using NRecon software (SkyScan NRecon version 1.7.4.6, Bruker). Misalignment compensation, ring artefacts and beam hardening were adjusted to obtain a correct reconstruction of the entire knee joint. Bone parameters were quantified using CTAn software (version 1.17.7.2, Bruker). No substantial disparities were identified in the histomorphometric assessment of femurs and tibias. Consequently, the single analysis of tibias is reported here. As bone sclerosis is generally observed in the medial epiphysis [16], the boundary between the subchondral bone plate and the trabecular subchondral zone is not easy to draw, making it difficult to measure bone parameters in the subchondral bone plate on this side. Therefore, we analysed two different bone regions: the lateral subchondral bone plate and the medial and lateral epiphyses of each tibia. Periarticular osteophyte formation and meniscus/ligament calcification were quantified on whole knee joints. Reconstructed 3D images of the joints were obtained using Avizo Lite software (version 2019.3, FEI).

Contrast-enhanced µCT analyses

For each hind paw, the tibia and femur were separated and the smooth tissues were carefully removed to expose the articular cartilage. Tibiae were incubated in a solution of 1% phosphotungstic acid (PTA) (a soft tissue radiopaque stain) in 70% ethanol for 24 h at room temperature and scanned in the µCT system (SkyScan 1176, Bruker) in the same solution. Images were acquired using the following parameters: 0.5 mm aluminium filter, 50 kV, 500 µA, 9 µm pixel size and 0.3° rotation angle. Images were then reconstructed using NRecon software (SkyScan NRecon version 1.7.4.6, Bruker). Misalignment compensation, ring artefacts and beam hardening were adjusted to obtain a correct reconstruction of the tibia.

Articular cartilage degradation was assessed using CTAn in two manually selected regions of interest (ROIs) of 800 µm length on the medial and lateral plateaus of each tibia. The ROI is delineated by extending mappings from the beginning of the separation between the lateral and median epiphyses towards 800 µm along the posterior-anterior axis. Quantitative analysis of cartilage volume, thickness and surface degradation was assessed in both ROIs using CTAn. Fixed knee joints were washed with 70% ethanol to remove PTA and stored in 70% ethanol at 4 °C for further analysis.

Confocal laser scanning microscopy

To image articular cartilage over the entire tibial medial and lateral plateaus, tibiae were imaged using a confocal laser scanning microscopy (CLSM), as previously described [17]. Briefly, the articular cartilage of each tibial plateau was scanned separately through its depth in XYZ-mode using CLSM (TCS SP5-II, Leica Microsystems). The following parameters were used to image each specimen: 5×dry objective, UV laser light source (l¼ 405 nm), detector gain of 800 V and line average of 5. For each sample, cartilage autofluorescence was acquired at every 5 µm of depth. The resulting image stack was used to reconstruct 3D images of each plateau, which were analysed to quantitatively assess articular cartilage volume, thickness and surface degradation. Cartilage morphometric parameters were assessed in both the lateral and medial plateaus of each tibia using Avizo Lite software (version 2019.3, FEI).

Histological analysis

After CLSM analysis, tibiae were decalcified in EDTA solution for three weeks and processed for histology. Samples were embedded in paraffin and frontal sections of 7 µm were cut. Three sections per sample were taken at different depths and mounted on a single slide. The first section was made at 50 µm below the cartilage surface; the second was taken at 100 µm below and the third at 100 µm below. Sections were stained with Safranin O/Fast Green to analyse cartilage. Cartilage degradation was quantified for the lateral and medial tibial plateaus using the modified Pritzker OsteoArthritis Research Society International (OARSI) score by grading and staging each degradation as described [18]. Three sections of each specimen were graded and the maximum score was assigned to the specimen. The minimum score is 0, indicating no cartilage or bone damage, whereas 30 is the maximum score indicating significant cartilage and bone degradation. Synovial activation scoring was performed on the entire knee joints sampled on days 9 and 28 using an arbitrary scoring from 0 (healthy synovium) to 3 (maximal extensive inflammation) according to synovial thickness as previously described [19]. Three sections of each specimen were scored and the mean score was assigned to the sample.

Statistical analyses

Statistical analyses and graphs were performed using the GraphPad Prism 8 software. For structural analyses (µCT, CLSM, histology), data are expressed as the mean ± SEM (standard error of the mean). Normal distribution and homogeneity of variance were determined using the Shapiro–Wilk and Fisher test followed by the one-tailed Mann–Whitney or unpaired t-test. Statistical analysis compared the non-injected or saline-injected control groups with the OA group.

For functional analyses, data are expressed as the mean ± SEM of the parameter measured in individual mouse (open field) or as the ratio between the injected leg (right hind or RH) and the contralateral intact leg (left hind or LH) (Catwalk™), except for the base of support parameter (distance between the left and right hind paws). Data were analysed by repeated two-way ANOVA (time and treatment effects) followed by post-hoc Tukey's multiple comparison test.

For mathematical correlations, data obtained from all groups at the most representative time point were pooled and the Pearson r coefficient was calculated for each pair of parameters. For the open field and catwalk data, the D9 time point was selected due to its position as the later time point at which statistical differences between the control and OA groups were observed. This time point was selected to ensure sufficient distance from the OA induction times (D0 and D2), thereby excluding the possibility of early local inflammation induced by the injection itself from influencing the results. For µCT and CLSM analysis, the D42 time point was selected because the scanning was conducted on joints after euthanasia.

For linear regressions, data obtained from all groups were pooled. Each functional parameter was plotted as a function of histological score. The linear equations obtained were used to calculate the theoretical value of the parameter for each histological score. The theoretical value obtained for a null histological score was taken as the reference. We then calculated the relative functional or structural deficit (expressed in %) for each parameter according to the formula: "relative deficit = (reference—theoretical value for each histological score)/reference × 100". Finally, we plotted these relative functional or structural deficits as a function

of histological score (expressed as % of the maximum score).

Results

OA induction causes transient locomotor deficits

To characterise motor deficits in the CIOA model, we longitudinally assessed locomotor parameters in control (Ctrl) mice and OA mice for 42 days. Two groups of OA mice were included: one group was given a running wheel (OA + W) to assess the effect of free exercise on the development of OA and the other group had no access to a wheel (OA-W). Two non-invasive and operator-independent locomotor tests were used: the open field to quantify global locomotor activity, and the Catwalk™ system to measure fine dynamic gait patterns. The Catwalk™ setup allows the quantification of several parameters related to gait and individual paw prints during spontaneous locomotion.

All the parameters measured with the open field test, i.e. total distance travelled, rest time, mean speed and time spent in fast movements were statistically different in the two OA groups compared to Ctrl mice at the very early time points (D3, D7 and D9) after OA induction (Fig. 1A). The most significant effect was observed at D3, with highly significant changes for all of these parameters. These effects persisted until D7 or D9, depending on the parameter and were abolished from D13 onwards. The differences observed in the total distance travelled and the rest time are illustrated by the plot of the total trajectory course of Ctrl and OA mice (Fig. 1B).

Among the parameters assessed by the Catwalk™ setup, we selected stance time, swing time, print area, duty cycle and base of support for hind paw as the most representative examples (Fig. 1C). These parameters were statistically different in the two OA groups compared to Ctrl mice only at D3, with no significant change observed at D9 and D29. On the contrary, the base of support (distance between the left and right hind paws) was significantly decreased in the two groups of OA mice compared to Ctrl mice from D9 till D29 as shown in Fig. 1C-D. Taken together, these results show that OA induction is associated with motor changes mainly at the early time points, changes that can persist for a few days before returning to normal baseline values.

OA leads to bone changes and abnormal calcification in the knee joints

To assess structural changes, bone changes were monitored by µCT at euthanasia on D42, which is the classical endpoint for CIOA evaluation [20]. The analysis of bone changes was performed on the three groups of mice that had been longitudinally evaluated for locomotor parameters (Ctrl mice, OA + W and OA-W mice). Severe abnormal calcification of the joints including the patella, menisci, and lateral and medial ligaments was observed in the knee joints of both OA groups compared to the Ctrl group (Fig. 2A). To quantify the bone changes and to assess the effect of free exercise on their severity, bone histomorphometric parameters were analysed in two different bone regions: the lateral subchondral bone plate and the medial and lateral epiphyses. In the lateral subchondral bone plate of OA mice, bone degradation occurred as indicated by a significant reduction in bone volume and thickness, accompanied by a significant increase in bone surface degradation (BS/BV parameter) compared to Ctrl mice (Fig. 2B). These results were correlated with a significant decrease in bone volume (BV/TV) in the lateral and medial epiphyseal regions of OA mice compared to control (Fig. 2C). Similar bone loss in these regions was observed between OA mice with free access to wheels for exercise and mice in cages without wheels. Although some OA mice developed bone sclerosis in the epiphyseal region, no significant difference was observed between OA and control mice (Fig. 2C). In contrast, bone loss was associated with a lower bone volume (BV/TV) in the total trabecular volume (TV) in the epiphysis and lower trabecular number and thickness (Fig. 2D). Finally, a significant increase in periarticular marginal osteophyte volume was quantified in both OA groups (Fig. 2E). The bone volume and the surface area of abnormal joint calcifications were also significantly increased in both groups of OA (Fig. 2F). We confirm here that severe bone changes occur during CIOA, regardless of whether the mice were offered free exercise or not.

OA causes severe articular cartilage degradation

Three distinct techniques were employed to image and quantify articular cartilage lesions in the three groups of mice euthanized on day 42, which had been longitudinally evaluated for locomotor parameters (Ctrl mice, OA + W and OA-W mice). Articular cartilage was first imaged by contrast-enhanced µCT after incubation of the tibiae in PTA. After incubation, the articular cartilage from the lateral and medial tibial plateaus was imaged by µCT as a radiopaque layer. The articular cartilage layer was intact in both tibial plateaus of Ctrl mice as indicated by the white arrows on a representative image in one mouse (Fig. 3A). Conversely, a thinner cartilage layer and zones of erosion were observed in the representative images of the two groups of OA mice, as indicated by the stars (Fig. 3A, middle and right panels). To quantify the articular cartilage degradation, several histomorphometric parameters were assessed on the tibial plateau of each mouse. A significant reduction in the mean thickness and volume along with a significant increase in the mean surface degradation were observed in both groups

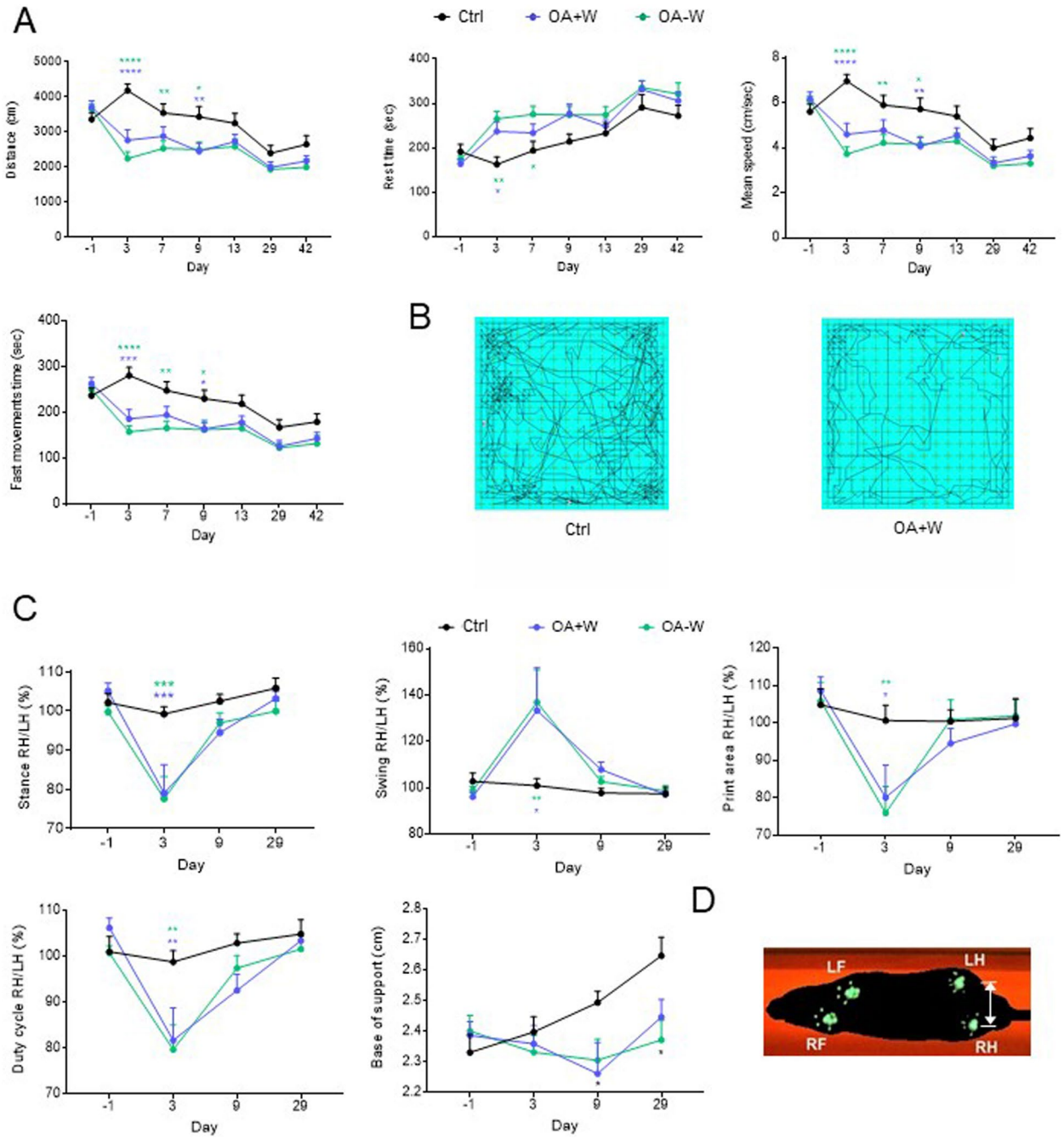

Fig. 1 Longitudinal monitoring of locomotion in CIOA mice. **A** Global locomotion measured in the open field for control (Ctrl, black dots, $n = 10$) mice and CIOA mice, with (OA + W, blue dots, $n = 14$) and without free access to a running wheel (OA-W, green dots, $n = 14$). Measured parameters are: distance travelled, rest time, mean speed and time spent in fast movements (i.e. with a speed above 5 cm/s). **B** Representative trajectories of a Ctrl and CIOA mouse during a 10 min open field session. **C** Spontaneous locomotion and gait parameters measured with Catwalk™. The measured parameters stance, swing, print area and duty cycle are expressed as a ratio between the right hind paw (ipsilateral) and the left hind paw (contralateral) while the base of support of the hind paws is measured in cm. **D** Representative image of a Ctrl mouse captured with the Catwalk.™ setup, with each paw shown in green (LF: left front, LH: left hind, RF: right front, RH: right hind paws; the double arrow illustrates base of support). Results are expressed as mean ± SEM. Statistical analysis was performed using the repeated two-way ANOVA test followed by the Tukey's multiple comparison test; *$p < 0.05$, **$p < 0.01$, ***$p < 0.001$, ****$p < 0.0001$

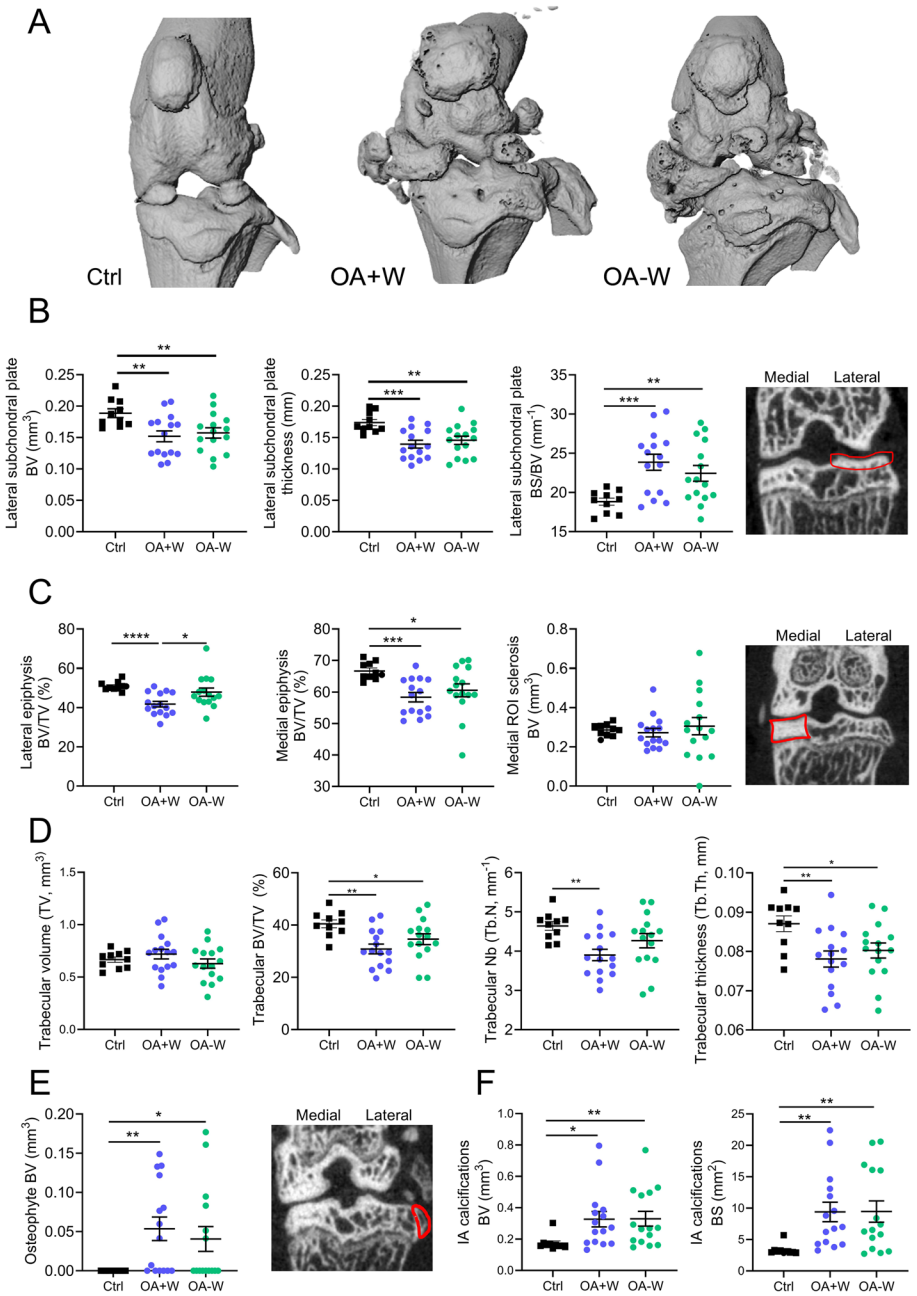

Fig. 2 Visualisation and quantification of bone changes in knee joints by µCT. **A** Representative 3D images of bone tissue in knee joints of control (Ctrl, $n=10$) mice and CIOA mice, with (OA + W, $n=14$) and without free access to a running wheel (OA-W, $n=14$) at day 42 (D42). **B** Histomorphometric analysis of the lateral subchondral bone plate (BV: bone volume, BS/BV: bone surface/bone volume; representative region in red in the right panel). **C** Histomorphometric analysis of the medial and lateral epiphysis (BV/TV: bone volume/tissue volume) and medial epiphysis sclerosis BV (bone volume) corresponding to the ROI illustrated in the right panel. **D** Histomorphometric analysis of epiphysis trabecular bone (trabecular volume BV/TV, trabecular number (Nb), trabecular thickness). **E** Histomorphometric analysis of osteophyte bone volume (BV) at the tibial margins, as illustrated in the right panel. **F** Histomorphometric analysis of calcifications in the joints (IA: intra-articular; BV: bone volume, BS: bone surface). Results are expressed as the mean ± SEM. Statistical analysis was performed using the unpaired t-test as compared to Ctrl mice with *: $p<0.05$; **: $p<0.01$; ***: $p<0.001$; ****: $p<0.0001$

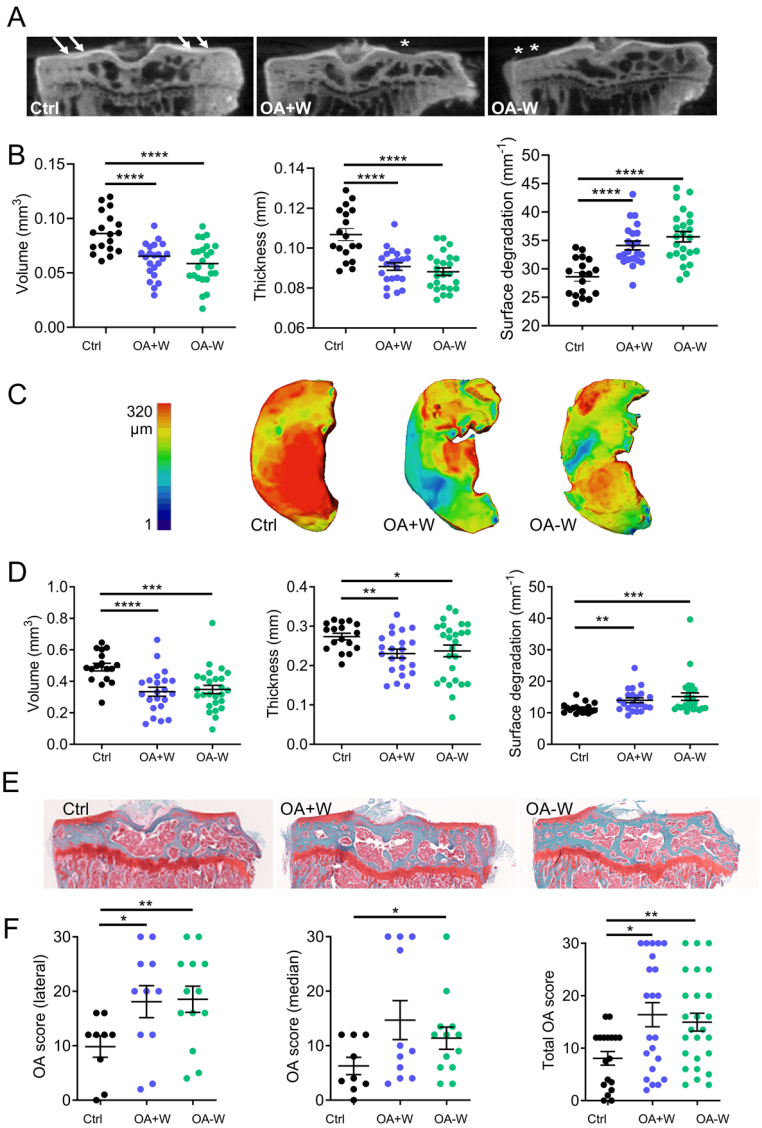

Fig. 3 Visualisation and quantification of articular cartilage changes in knee joints. **A** Representative coronal sections of the epiphyseal region from tibiae of control (Ctrl, $n = 10$) mice and ClOA mice, with (OA + W, $n = 14$) and without free access to a running wheel (OA-W, $n = 14$) obtained by contrast-enhanced µCT at day 42 (D42). Intact articular cartilage (blank areas) is visualised by white arrows and cartilage erosion with white stars. **B** Histomorphometric analysis of articular cartilage measuring thickness, volume and surface degradation (surface/volume). **C** Representative 3D images of medial tibial cartilage obtained by CLSM and a colour code (left) indicating the thickness from the border with the subchondral bone plate to the maximum cartilage surface in Ctrl mice. **D** Histomorphometric analysis of articular cartilage measuring thickness, volume and surface degradation. **E** Representative histological images of knee joints. **F** Histological OA score in lateral, medial and total (lateral + medial) compartments. The results are expressed as mean ± SEM. Statistical analysis was performed using Mann–Whitney test as compared to Ctrl with *: $p < 0.05$; **: $p < 0.01$; ***: $p < 0.001$; ****: $p < 0.0001$

of OA mice compared to Ctrl mice confirming cartilage loss (Fig. 3B).

The articular cartilage was then analysed using CLSM. This technique has the advantage of allowing accurate quantitative analysis of the cartilage in a full 3D cartography. Representative 3D images of the medial tibial plateaus showed important cartilage degradation in both groups of OA mice compared to Ctrl mice, as indicated by the erosion of the articular cartilage contour and the higher areas of blue and green regions, indicating reduced thickness (Fig. 3C). The quantification of histomorphometric parameters of the two tibial plateaus in each mouse confirmed a significant decrease in the mean cartilage thickness and volume as well as a significant mean increase in the surface degradation in both OA groups versus the Ctrl group (Fig. 3D).

Finally, histological analysis of the knee joints was used as this technique is considered as the reference method for visualizing and quantifying cartilage degradation in OA models, notably in CIOA [20]. The histological OA score, reflecting cartilage degradation, was significantly increased in the lateral and medial plateaus in both OA groups compared to the Ctrl group at day 42 (Fig. 3E-F). For both plateaus, cartilage degradation was equivalent in the knee joints of mice with and without free wheel access.

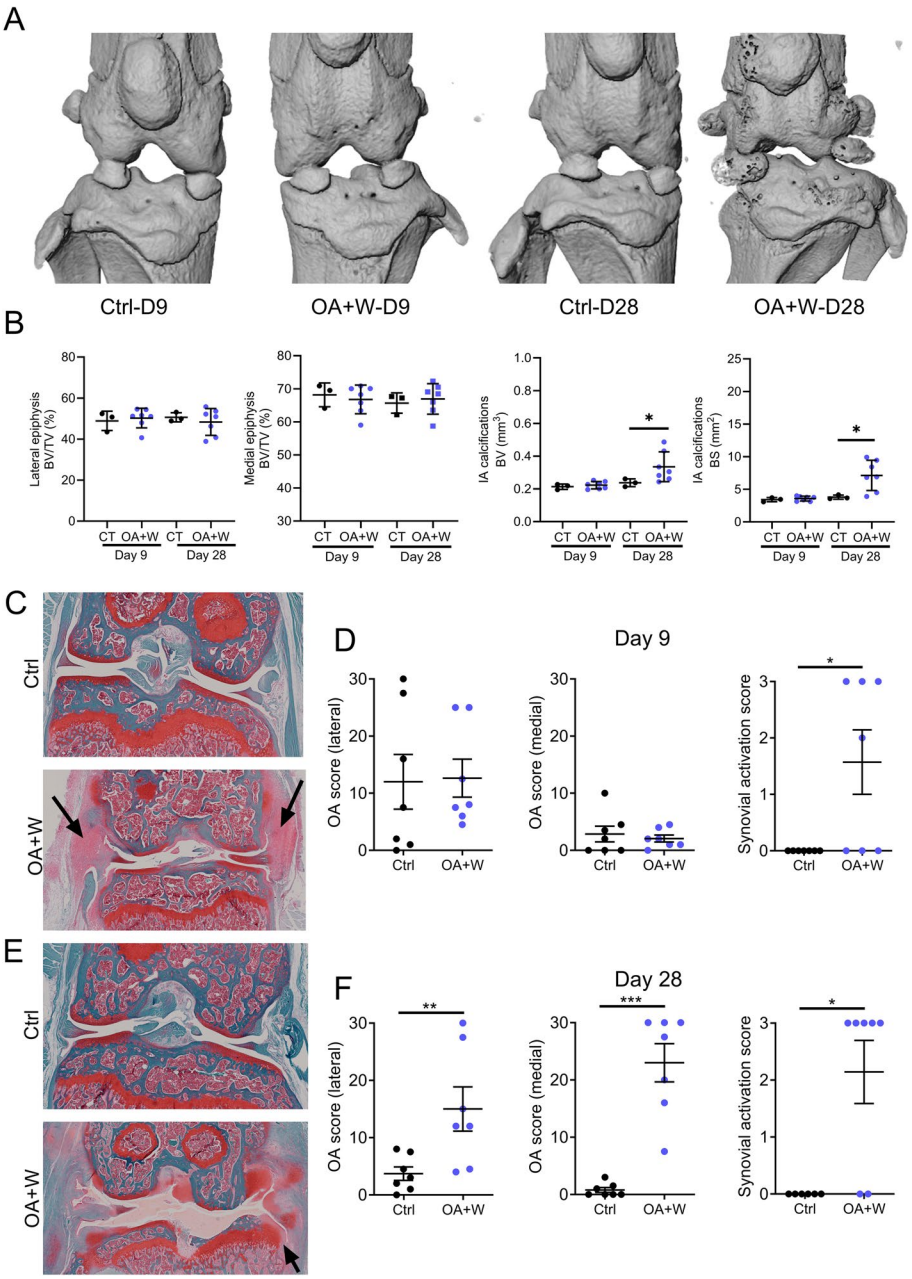

Fig. 4 Analysis of knee joints in CIOA mice at early time points. **A** Representative 3D images of bone tissue in knee joints of control (Ctrl, $n=7$) mice and CIOA mice with free access to a running wheel (OA + W, $n=7$) on days 9 and 28 (D9 and D28). **B** Histomorphometric analysis of the medial and lateral epiphysis (BV/TV: bone volume/tissue volume) and, calcifications in the joints (IA: intra-articular; BV: bone volume, BS: bone surface). **C** Representative histological images of knee joints from Ctrl and OA + W groups at D9. **D** Histological OA score in lateral and medial compartments and synovial activation score at D9. **E** Representative histological images of knee joints of Ctrl and OA + W groups at D28. **F** Histological OA score in lateral and medial compartments and synovial activation score at D28. Arrows show synovial inflammation. Results are expressed as mean ± SEM. Statistical analysis was performed using the Mann–Whitney test as compared to Ctrl with *: $p<0.05$; **: $p<0.01$; ***: $p<0.001$

Two additional groups of OA mice (OA + W) and Ctrl mice have been included and euthanised at earlier time points (D9 and D28). Only histological scores and µCT analysis were performed on these mice. At day 9, µCT analysis revealed no major difference between the OA mice and the Ctrl mice (Fig. 4A). However, by day 28, calcification of the menisci and ligaments were clearly evidenced in the OA group indicating early bone formation in the soft tissues of the joint. A significant increase in calcifications of the knee joints was observed at day 28, but not at day 9. No alterations in the epiphyseal bone were detected at either time point (Fig. 4B). Severe inflammation of the synovial membrane was observed in the OA + W group on day 9 (Fig. 4C, arrows). This observation correlates with a significant increase in the synovial activation score in these mice compared to Ctrl mice with no significant increase in the histological score (Fig. 4D). By contrast, cartilage degradation of both plateaus was observed in the OA + W group at day 28 (Fig. 4E). Cartilage loss was confirmed by the significant increase in the histological score in both plateaus and inflammation was illustrated by the high synovial activation score (Fig. 4F). Similar results were obtained with the different techniques, but contrast-enhanced µCT and, more globally, CLSM allow both 3D visualisation of the cartilage tissue and quantification of several histomorphometric parameters throughout the cartilage at the surface of long bones with less bias than operator-dependent histological scoring.

Functional and structural deficits are correlated with the histological score

With the hypothesis that the structural and locomotor deficits observed in OA mice are correlated with the histological score, the standard technique for assessing OA, mathematical correlations were performed between the different parameters quantified by each technique and the histological score. A correlation coefficient was considered to be relevant if it was around or above 0.5 and around or below −0.5.

For locomotor deficits, a high correlation was found between all the parameters measured within each of the two techniques, the open field and the Catwalk™, confirming that these parameters are accurate in detecting the same phenomenon (Fig. 5A-B). For the open field, relevant correlation coefficients were obtained between the histological score of the medial tibia and the four parameters of i.e. distance ($r=-0.54$), mean speed ($r=-0.54$), fast movements ($r=-0.53$) and rest time ($r=0.51$) (Fig. 5A). This indicates that low values for distance, mean speed and time spent in fast movements and increased rest time are associated with a high histological score, particularly in the medial tibia. For the Catwalk™ parameters, only the maximal intensity of the paw print was found to correlate with the histological score of the medial tibia ($r=-0.48$) (Fig. 5B).

For structural analysis, several bone parameters assessed by µCT correlated with each other. High bone volume (BV/TV) in the lateral and median epiphyses correlated with low osteophyte volume and intra-articular calcification volume (Fig. 5C). A relevant inverse correlation was obtained between the bone volume of the lateral epiphysis (BV/TV) and the histological scores in the lateral tibiae ($r=-0.53$). Finally, all cartilage parameters assessed by both techniques, contrast-enhanced µCT and CLSM, were highly correlated as the volume and thickness of cartilage were inversely correlated with surface degradation (Fig. 5D-E). Furthermore, a relevant correlation between the medial cartilage volume and the histological score of the lateral and medial tibiae ($r=-0.42$ and $r=-0.59$, respectively) was found by enhanced-contrast µCT (Fig. 5D). CLSM showed a significant correlation between the medial volume and surface degradation of cartilage and the histological score of the medial tibia ($r=-0.51$ and $r=0.53$, respectively) (Fig. 5E). Taken together, all these data suggest that both locomotor and structural parameters are correlated with post-mortem histological scores. In particular, locomotor deficits assessed by open field and bone structural changes by µCT, which are both non-destructive techniques, could be used to predict the severity of OA.

A new tool to predict histological score from locomotor or structural deficits

We then wanted to find out which technique and which parameters were the best predictors of OA development. To do this, parameters of general locomotion, gait analysis, bone structure and cartilage structure were plotted as a function of the histological score after pooling all time points and all groups for each technique. The relative functional or structural deficit was then calculated for each parameter and the linear equations of these deficits were plotted as a function of the relative histological score. Interestingly, the linear regression slopes for the global locomotor parameters quantified by open field analysis overlapped very well, meaning that each parameter was equally efficient at predicting the histological scores (Fig. 6A). For gait analysis using the Catwalk™ setup, the stance and print area parameters were the most affected parameters, suggesting that they can predict the histological score quite well (Fig. 6B). For example, a 30% motor deficit measured by either the open field parameters or the Catwalk™ stand parameter would predict an 80% cartilage change measured by the histological score. For µCT analysis, bone volume of periarticular osteophytes and calcification of ligaments

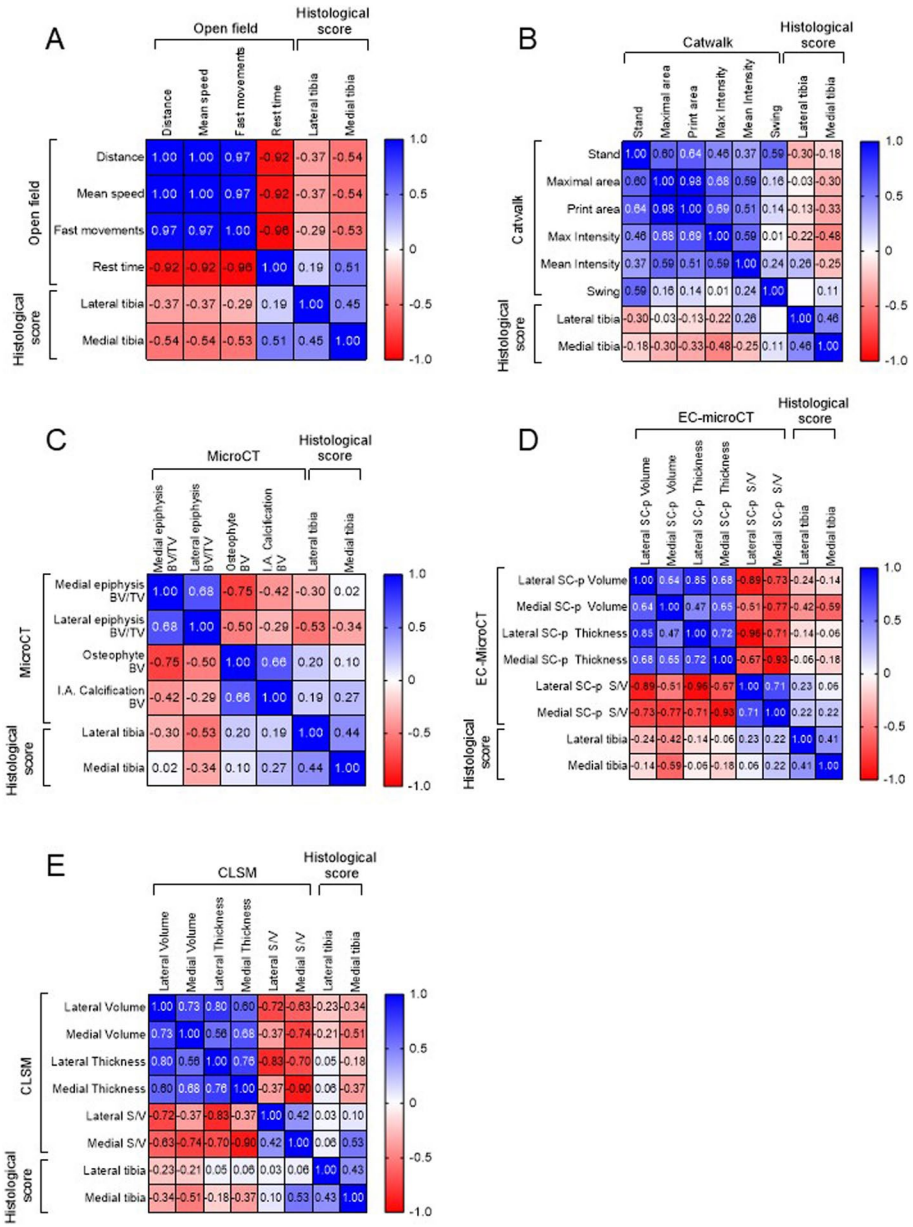

Fig. 5 Correlations between histological score and functional or structural parameters. **A** Heatmap of the Pearson correlation matrix between histological score of lateral and medial tibia and global locomotor parameters measured with open field. **B** Heatmap of the Pearson correlation matrix between histological score of lateral and medial tibia and paw print parameters measured with Catwalk.™. **C** Heatmap of the Pearson correlation matrix between histological score of lateral and medial tibia and bone structure parameters measured by µCT. **D** Heatmap of the Pearson correlation matrix between histological score of lateral and medial tibia and cartilage structural parameters measured by contrast-enhanced µCT on lateral and medial compartments. **E** Heatmap of the Pearson correlation matrix between histological score of lateral and medial tibia and cartilage structural parameters measured by CLSM on lateral and medial compartments. BV: Bone volume, TV: Tissue volume, µCT: micro-computed tomography and EC-µCT: contrast-enhanced µCT, CLSM: confocal laser scanning microscopy, SC-p: Sub-chondral plate; S/V: surface/volume. The values given in each matrix cell correspond to the Pearson r correlation coefficient ($n = 31$)

and meniscus appear to be better predictors of histological degradation than lateral epiphysis BV/TV (Fig. 6C). For cartilage analysis, the linear regression slopes for some parameters (volume and surface/volume ratio of the medial cartilage plate) measured by both techniques, enhanced-contrast µCT and CLSM, overlapped very well suggesting that both techniques are highly comparable and that each parameter can also predict the histological score (Fig. 6D). We therefore propose that these new data could be used as new scales to predict histological

changes simply by longitudinally measuring locomotor and bone deficits in CIOA.

Finally, to confirm that locomotor parameters can predict OA severity, the most reliable parameters were separated by histological score, divided into low (0 to < 15) and high (≥ 15 up to 30) grade OA. We found that all global locomotor parameters were indicative of OA severity: the distance, mean speed and time spent in fast movements were significantly decreased, whereas rest time was significantly increased with the highest histological scores (Fig. 6E). For gait parameters, stand time and print area of the right hind paw (OA induced), as well as the distance between the intact (left hind paw) and the right hind paw (base of support) were significantly decreased with high histological score. Overall, these data confirm that locomotor and structural deficits are correlated and predictive of histological changes measured postmortem.

Discussion

In this study, we provide evidence that global locomotion and gait assessment are altered in the CIOA-induced mice at early time points after OA induction. These locomotor deficits are associated with structural changes in articular cartilage and bone and correlate with histological score, the standard for assessing OA.

To the best of our knowledge, this is the first study to evaluate in depth both locomotor, pain and structural deficits in the CIOA model. Several types of tests have been used to assess locomotor and pain deficits, including the rotarod, hotplate, open field, and gait analysis in different models of OA [21]. Here we used two complementary and sensitive tests, Catwalk™ and open field. Open field analysis showed significant changes in distance, rest time, mean speed and fast movements time parameters from D3 to D9 after OA induction. The changes were not due to injection-related pain, as the control mice also received a saline injection. Similar to our findings, decreased distance and increased rest time have been reported in mice with CIOA [22]. However, no differences were observed in the transection of anterior cruciate ligament (ACTL) or DMM induced OA mice when open field was performed either at 4 weeks [23] or every 2 weeks from week 2 [24]. This suggests that open field is a relevant test for assessing CIOA-associated pain in the early stages, and its interest needs to be confirmed in other OA mouse models soon after induction. For the Catwalk™ analysis, the stand, swing, print area, duty cycle and BOS parameters were the most significantly affected parameters at day 3 after OA induction but they recovered by D9, as also reported in the ACTL and CIOA mouse models [25, 26]. In the DMM model, no gait impairment was observed when looking at the intensity of the paw print parameter [27], which is consistent with our study (data not shown). In another study, no significant changes of locomotor parameters were seen from week 3 to week 8 after DMM surgery but they were altered from week 12 to week 16 [28]. In fact, assessment of locomotion was performed at different time points depending on the study, which may explain the differences observed. Nevertheless, all these results suggest that locomotion is affected during the first week of OA onset and after a period of recovery, pain and locomotor deficits may recur at later time points, which would be worth investigating in further studies.

Structural analysis of knee joints includes µCT for visualisation and quantification of bone parameters and enhanced-contrast µCT and CLSM for measurement of cartilage parameters as described [7, 17]. Bone analysis often quantifies bone parameters in the subchondral bone plate and in the epiphysis. In the present study, bone volume as measured by the BV/TV parameter is decreased in both compartments while surface degradation as measured by the BS/BV parameter is increased, which is often observed in the CIOA model [13, 15, 29]. Decreased BV/TV is also associated with reduced trabecular number and thickness [30]. While bone sclerosis is generally quantified by measuring subchondral bone plate thickening [16], this can be difficult to measure when the sclerosis is severe, which is the case in a small number of animals in our study. We therefore

(See figure on next page.)

Fig. 6 Prediction of histological score based on assessment of locomotor and structural deficits. **A** Relative global locomotor deficits (% of maximum) measured in the open field as a function of relative maximum histological score. **B** Relative gait locomotor deficits (% of maximum) measured by Catwalk™ as a function of relative maximum histological score. **C** Relative structural changes in bone (% of maximum) measured by µCT as a function of relative maximum histological score. Lateral epiphysis BV/TV and Calcifications of ligaments and meniscus BV are plotted on the left Y-axis, Osteophytes BV is plotted on the right Y-axis. **D** Relative structural changes in cartilage (% of maximum) measured by EC-µCT or CLSM as a function of relative maximum histological score. MP: Medial subchondral plate, S/V: Surface/Volume ratio, µCT: Micro-Computed Tomography, EC-µCT: contrast-enhanced µCT, CLSM: Confocal Laser Scanning Microscopy, BV: Bone Volume, TV: Tissue Volume. **E** Open field parameters (distance, mean speed, fast movements and rest time expressed relative to OA severity as assessed by histological score (HS). **F** Catwalk.™ parameters (stance, print area, base of support for hind paws and swing for right hind paw) are expressed relative to OA severity of the RH paw as assessed by histological score. Data from all experimental groups were pooled and results are expressed as the mean ± SEM. Statistical analysis was performed using an unpaired bilateral t-test or a Mann–Whitney test depending on data normality; *: $p < 0,05$

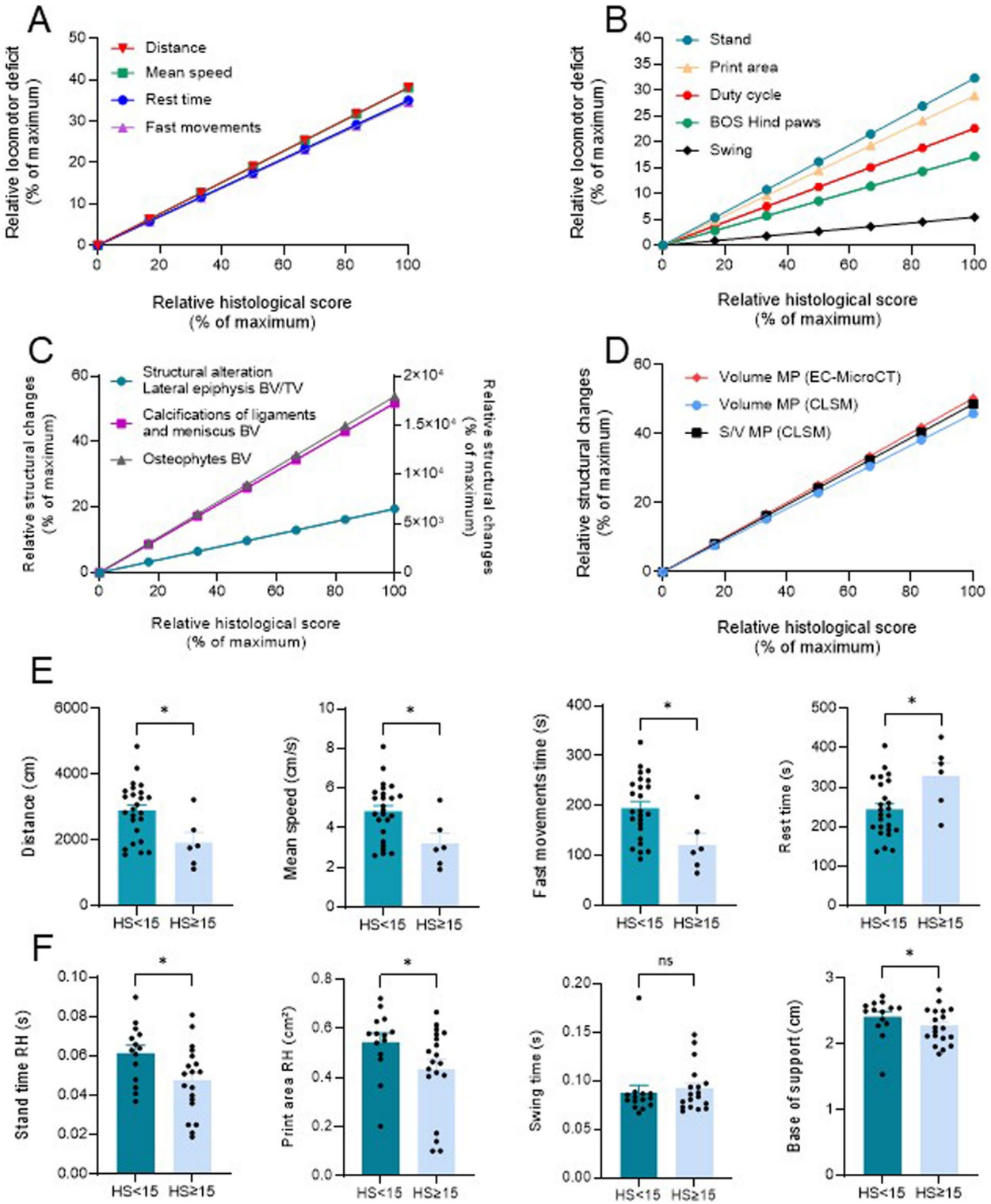

Fig. 6 (See legend on previous page.)

measured the sclerosis in a region of interest in the epiphysis as a more accurate parameter (shown in Fig. 2C), as also reported [31]. Importantly, severe changes in the knee joint including meniscal calcifications as shown by meniscal ossicles are associated with OA in both the CIOA and DMM models [15, 31]. Interestingly, meniscal

calcifications were observed as early as day 28, but given the importance of calcifications, we hypothesise that these changes could be observed earlier. This structural parameter is therefore important for the prediction of OA development as discussed below.

Clinical studies consistently recommend exercise as a treatment for OA, and this is supported by the slowing of OA progression in rodents. Several studies have shown that gentle or moderate exercise has a beneficial effect on OA, while high-intensity exercise is detrimental [32]. A recent study reported that forced moderate exercise on rotating wheels provides protection against cartilage damage using the destabilisation of the medial meniscus (DMM) mouse model [33]. However, conflicting results have been reported on the effect of voluntary wheel running on the progression of OA. While wheel running was shown to reduce the OA score in the medial femur in a high-fat diet-induced mouse model of OA [34], it was reported to have minimal effect on OA progression with only a reduction in trabecular BMD in obese mice [35]. Although the CIOA model is not associated with major metabolomic changes, severe synovial inflammation is a common symptom in both models that triggers the development of OA. One obvious difference is the exercise regimen and it is unlikely that mild or moderate exercise has the same effect on OA development. Further studies are needed to elucidate the underlying mechanisms.

Interestingly, we found relevant correlations between some functional and structural parameters and the histological scores. First, the correlation coefficients measured within each technique are very high (around −1 or + 1) for closely related parameters (e.g. distance, mean speed, time spent in fast movements and rest time measured with the open field test or print area and maximum contact area for Catwalk™), which means that within each technique the parameters are very consistent with each other and that one parameter could be helpful in predicting the behaviour of the others. Second, the histological score can be correlated with a number of selected parameters measured by different techniques that assess either functional or structural deficits. A few studies have examined possible correlations between histological and structural or behavioural parameters. In the CIOA model, a correlation was reported between pain-related parameters measured by Catwalk™ and histological evaluation of cartilage damage and osteophyte number [26]. The correlation was mainly observed in females and poorly in males although there is a predominant consensus that OA is more prevalent in males [36]. In agreement, our study realized with males shows weak correlations, except for the max intensity parameter. These results suggest that the Catwalk™ test cannot predict cartilage damage as evaluated by histological score although we cannot rule out that different types of analysis (individual area under the curve for each parameter pooled from different cohorts versus raw data for each parameter in our cohort) may lead to different results.

The correlations obtained in our study suggest that locomotor and structural parameters could be predictive of the severity of the pathology. Therefore, additional mathematical calculations were performed to express the relative locomotor or structural deficits as a function of the relative histological scores and to compare the linear regression curves obtained for each technique. The curves obtained for the four parameters evaluated using the open field test were almost superimposable, underlining the robustness of our results and the equivalence of each parameter to predict the histological score, and therefore the severity of OA. By contrast, the results obtained with Catwalk™ are dependent on the parameters measured, with the stance time and print area being the parameters most affected by the progression of OA. Relevance of these parameters is also indicated by their capacity to classify OA mice in low or high grade groups. For cartilage assessment, both enhanced-contrast μCT and CLSM are highly comparable in predicting the histological score while for bone assessment, the volume of periarticular osteophytes measured by μCT is highly predictive of OA. Such mathematical prediction has already been performed for another mouse model of osteoarticular disease, namely the collagen-induced arthritis model [37]. In this model of experimental arthritis, the distance (measured with the open field test) and the print area (measured with the Catwalk™) are very comparable for predicting the severity of inflammatory arthritis. In CIOA, the distance and mean speed parameters (open field) were more responsive (40%) to a modification of the histological score than the most affected parameters stand or print area (Catwalk™) (30%), suggesting that the open field test is more sensitive to evaluate locomotor deficits and more predictive of cartilage damage in CIOA. Nevertheless, the best scores (50%) were obtained with contrast-enhanced μCT and CLSM for cartilage evaluation. This is not surprising since the histological score is mainly based on the evaluation of cartilage degradation. However as discussed elsewhere, the pain-structure relationship in OA is very complex and pain, frequently associated with locomotor deficits, is not always correlated with structural deficits [38]. Synovial inflammation, which translates in pain, plays a major role in CIOA induction. We show here severe synovitis in OA mice at day 9, which is likely reflected by the locomotor deficits measured from day 3 to day 9. How pain translates in the CIOA model and how functional deficits contribute to OA development has still to be evaluated.

Conclusions

All together, these tools allow us to recommend the follow-up of some predictive factors of OA at different time points during the course of the disease. Functional deficits should be better evaluated using the open field test during the first two weeks and measuring any parameter among distance, rest time, man speed or fast movements time. Structural deficits can be monitor as soon as day 28 (and likely earlier) by µCT to observe intra-articular calcifications and periarticular osteophyte formation at the femoral or tibial epiphyses. These two techniques are neither destructive nor invasive and allow the longitudinal evaluation of mice induced to develop OA in a relatively short period of time. Importantly, longitudinal evaluation is in line with the 3Rs principles for the ethical use of animals in science, which aim to reduce the number of animals used in experiments.

Supplementary Information

The online version contains supplementary material available at https://doi.org/10.1186/s13075-025-03507-w.

Supplementary Material 1. Linear regressions between representative functional or structural parameters and histological scores. A) Time spent in fast movements measured in the open field as a function of medial tibia's histological score. B) Maximal intensity of the right hind (RH) paw print measured by Catwalk^{TM} as a function of medial tibia's histological score. C) Lateral epiphysis bone volume/tissue volume measured by µCT as a function of lateral tibia's histological score. D) Medial cartilage volume measured by CLSM as a function of medial tibia's histological score. E) Cartilage surface/volume measured by CLSM as a function of medial tibia's histological score. S/V: Surface/Volume ratio, µCT: Micro-Computed Tomography, CLSM: Confocal Laser Scanning Microscopy, BV: Bone Volume, TV: Tissue Volume. Control mice (Ctrl, black dots, n=8) and CIOA mice (OA, green dots, n=24) are gathered on the same graph. The coefficient of determination R^2 is mentioned besides the linear regression. Statistical analysis was performed to test if the slope of the regression line is different to zero; **: p<0,01; ***:p<0.001.

Acknowledgements

We acknowledge support from the Inserm Institute, the University of Montpellier and the University Hospital of Montpellier. We gratefully acknowledge the Montpellier Histology Network (RHEM) for tissue processing and the OsteoStart platform for functional phenotyping of the animals. We also thank the Network of Animal facilities of Montpellier (RAM) for taking care of the animals.

AI declaration

The authors declare that they have not use AI-generated work in this manuscript.

Authors' contributions

Concept and design: CJ, DN, KT, ALB. Acquisition: KT, ALB. Analysis and interpretation of data: KT, ALB, DN. Drafting and critical revision of the article: KT, ALB, CJ, DN. Final approval of the article: KT, ALB, CJ, DN.

Funding

We acknowledge the Agence Nationale pour la Recherche for support of the national infrastructure: "ECELLFRANCE: Development of a national adult mesenchymal stem cell-based therapy platform" (PIA-ANR-11-INSB-005). This work benefited from state aid managed by the Agence Nationale de la Recherche under the France 2030 programme, under the references"ANR-22-PEBI-0013" , "ANR-22-PEBI-0002" and "ANR-22-AIBB-0007".

Data availability

All datasets generated or analysed during the current study are included or available upon request.

Declarations

Ethics approval and consent to participate

Animal procedures were performed in an animal facility certified by the French health authorities (agreement D34-172–36) and in accordance with the European guidelines (Directive 2010/63/EU). This project entitled « Effet thérapeutique des cellules stromales mésenchymateuses par ingénierie tissulaire ou thérapie cellulaire dans l'arthrose" was approved by the Languedoc-Roussillon Animal Research Ethics Committee (CEEA-LR n°36) and the French Ministry of Higher Education and Research (approval APAFIS#5349–2016050918198875) on April 2022.

Consent for publication

The authors approved manuscript submission.

Competing interests

The authors declare no competing interests.

Author details

[1]IRMB, University of Montpellier, INSERM, 80 Avenue Augustin Fliche, Montpellier, France. [2]Clinical Immunology and Osteoarticular Disease Therapeutic Unit, Department of Rheumatology, CHU Montpellier, France.

Received: 23 October 2024 Accepted: 15 February 2025
Published online: 26 February 2025

References

1. Katz JN, Arant KR, Loeser RF. Diagnosis and Treatment of Hip and Knee Osteoarthritis: A Review. JAMA. 2021;325(6):568–78.
2. Longo UG, Papalia R, De Salvatore S, Picozzi R, Sarubbi A, Denaro V. Induced Models of Osteoarthritis in Animal Models: A Systematic Review. Biology (Basel). 2023;12(2):283–300.
3. van der Kraan PM, Vitters EL, van Beuningen HM, van de Putte LB, van den Berg WB. Degenerative knee joint lesions in mice after a single intra-articular collagenase injection. A new model of osteoarthritis. J Exp Pathol (Oxford). 1990;71(1):19–31.
4. Drevet S, Favier B, Lardy B, Gavazzi G, Brun E. New imaging tools for mouse models of osteoarthritis. Geroscience. 2022;44(2):639–50.
5. Blease A. Das Neves Borges P, Curtinha M, Javaheri B, von Loga IS, Parisi I, Zarebska J, Pitsillides A, Vincent TL, Potter PK: Studying Osteoarthritis Pathogenesis in Mice. Curr Protoc Mouse Biol. 2018;8(4): e50.
6. Pauwels E, Van Loo D, Cornillie P, Brabant L, Van Hoorebeke L. An exploratory study of contrast agents for soft tissue visualization by means of high resolution X-ray computed tomography imaging. J Microsc. 2013;250(1):21–31.
7. Neves Borges P. Das, Forte AE, Vincent TL, Dini D, Marenzana M: Rapid, automated imaging of mouse articular cartilage by microCT for early detection of osteoarthritis and finite element modelling of joint mechanics. Osteoarthritis Cartilage. 2014;22(10):1419–28.
8. Stok KS, Noel D, Apparailly F, Gould D, Chernajovsky Y, Jorgensen C, Muller R. Quantitative imaging of cartilage and bone for functional assessment of gene therapy approaches in experimental arthritis. J Tissue Eng Regen Med. 2010;4(5):387–94.
9. Jacobs BY, Allen KD. Factors affecting the reliability of behavioral assessments for rodent osteoarthritis models. Lab Anim. 2020;54(4):317–29.
10. Otis C, Gervais J, Guillot M, Gervais JA, Gauvin D, Pethel C, Authier S, Dansereau MA, Sarret P, Martel-Pelletier J, et al. Concurrent validity of different functional and neuroproteomic pain assessment methods in the rat osteoarthritis monosodium iodoacetate (MIA) model. Arthritis Res Ther. 2016;18:150.
11. Ouhaddi Y, Najar M, Pare F, Lussier B, Urade Y, Benderdour M, Pelletier JP, Martel-Pelletier J, Fahmi H. L-PGDS deficiency accelerated the development of naturally occurring age-related osteoarthritis. Aging (Albany NY). 2020;12(24):24778–97.

12. Fouasson-Chailloux A, Dauty M, Bodic B, Masson M, Maugars Y, Metayer B, Veziers J, Lesoeur J, Rannou F, Guicheux J, et al. Posttraumatic Osteoarthritis Damage in Mice: From Histological and Micro-Computed Tomodensitometric Changes to Gait Disturbance. Cartilage. 2021;13(2):1478S-1489S.
13. Cosenza S, Ruiz M, Toupet K, Jorgensen C, Noel D. Mesenchymal stem cells derived exosomes and microparticles protect cartilage and bone from degradation in osteoarthritis. Sci Rep. 2017;7(1):16214.
14. Maumus M, Manferdini C, Toupet K, Chuchana P, Casteilla L, Gachet M, Jorgensen C, Lisignoli G, Noel D. Thrombospondin-1 Partly Mediates the Cartilage Protective Effect of Adipose-Derived Mesenchymal Stem Cells in Osteoarthritis. Front Immunol. 2017;8:1638.
15. Ruiz M, Toupet K, Maumus M, Rozier P, Jorgensen C, Noel D. TGFBI secreted by mesenchymal stromal cells ameliorates osteoarthritis and is detected in extracellular vesicles. Biomaterials. 2020;226: 119544.
16. Das Neves Borges P, Vincent TL, Marenzana M: Automated assessment of bone changes in cross-sectional micro-CT studies of murine experimental osteoarthritis. PLoS One 2017, 12(3):e0174294.
17. Stok KS, Pelled G, Zilberman Y, Kallai I, Goldhahn J, Gazit D, Muller R. Revealing the interplay of bone and cartilage in osteoarthritis through multimodal imaging of murine joints. Bone. 2009;45(3):414–22.
18. Pritzker KP, Gay S, Jimenez SA, Ostergaard K, Pelletier JP, Revell PA, Salter D, van den Berg WB. Osteoarthritis cartilage histopathology: grading and staging. Osteoarthritis Cartilage. 2006;14(1):13–29.
19. Hayer S, Vervoordeldonk MJ, Denis MC, Armaka M, Hoffmann M, Backlund J, Nandakumar KS, Niederreiter B, Geka C, Fischer A, et al. "SMASH" recommendations for standardised microscopic arthritis scoring of histological sections from inflammatory arthritis animal models. Ann Rheum Dis. 2021;80(6):714–26.
20. Schelbergen RF, van Dalen S, Ter Huurne M, Roth J, Vogl T, Noel D, Jorgensen C, van den Berg WB, van de Loo FA, Blom AB, et al. Treatment efficacy of adipose-derived stem cells in experimental osteoarthritis is driven by high synovial activation and reflected by S100A8/A9 serum levels. Osteoarthritis Cartilage. 2014;22(8):1158–66.
21. Alves-Simoes M. Rodent models of knee osteoarthritis for pain research. Osteoarthritis Cartilage. 2022;30(6):802–14.
22. Liu R, Zhou Y, Chen H, Xu H, Zuo M, Chen B, Wang H. Membrane vesicles from Lactobacillus johnsonii delay osteoarthritis progression via modulating macrophage glutamine synthetase/mTORC1 axis. Biomed Pharmacother. 2023;165: 115204.
23. Chou YJ, Chuu JJ, Peng YJ, Cheng YH, Chang CH, Chang CM, Liu HW. The potent anti-inflammatory effect of Guilu Erxian Glue extracts remedy joint pain and ameliorate the progression of osteoarthritis in mice. J Orthop Surg Res. 2018;13(1):259.
24. Hwang SM, Feigenson M, Begun DL, Shull LC, Culley KL, Otero M, Goldring MB, Ta LE, Kakar S, Bradley EW, et al. Phlpp inhibitors block pain and cartilage degradation associated with osteoarthritis. J Orthop Res. 2018;36(5):1487–97.
25. Angeby Moller K, Aulin C, Baharpoor A, Svensson CI. Pain behaviour assessments by gait and weight bearing in surgically induced osteoarthritis and inflammatory arthritis. Physiol Behav. 2020;225: 113079.
26. Valdrighi N, Blom AB, van Beuningen HM, Vitters EL, Helsen MM, Walgreen B, van Lent P, Koenders MI, van der Kraan PM, van de Loo FAJ, et al. Early pain in females is linked to late pathological features in murine experimental osteoarthritis. PeerJ. 2023;11: e15482.
27. Malfait AM, Ritchie J, Gil AS, Austin JS, Hartke J, Qin W, Tortorella MD, Mogil JS. ADAMTS-5 deficient mice do not develop mechanical allodynia associated with osteoarthritis following medial meniscal destabilization. Osteoarthritis Cartilage. 2010;18(4):572–80.
28. Muramatsu Y, Sasho T, Saito M, Yamaguchi S, Akagi R, Mukoyama S, Akatsu Y, Katsuragi J, Fukawa T, Endo J, et al. Preventive effects of hyaluronan from deterioration of gait parameters in surgically induced mice osteoarthritic knee model. Osteoarthritis Cartilage. 2014;22(6):831–5.
29. Malaise O, Tachikart Y, Constantinides M, Mumme M, Ferreira-Lopez R, Noack S, Krettek C, Noel D, Wang J, Jorgensen C, et al. Mesenchymal stem cell senescence alleviates their intrinsic and seno-suppressive paracrine properties contributing to osteoarthritis development. Aging (Albany NY). 2019;11(20):9128–46.
30. Cheng JH, Chou WY, Wang CJ, Siu KK, Peng JM, Wu YN, Lee MS, Huang CY, Ko JY, Jhan SW. Pathological, Morphometric and Correlation Analysis of the Modified Mankin Score, Tidemark Roughness and Calcified Cartilage Thickness in Rat Knee Osteoarthritis after Extracorporeal Shockwave Therapy. Int J Med Sci. 2022;19(2):242–56.
31. Rosch G, Muschter D, Taheri S, El Bagdadi K, Dorn C, Meurer A, Zaucke F, Schilling AF, Grassel S, Straub RH, et al. beta2-Adrenoceptor Deficiency Results in Increased Calcified Cartilage Thickness and Subchondral Bone Remodeling in Murine Experimental Osteoarthritis. Front Immunol. 2021;12: 801505.
32. Manninen P, Riihimaki H, Heliovaara M, Suomalainen O. Physical exercise and risk of severe knee osteoarthritis requiring arthroplasty. Rheumatology (Oxford). 2001;40(4):432–7.
33. Huesa C, Dunning L, MacDougall K, Fegen M, Ortiz A, McCulloch K, McGrath S, Litherland GJ, Crilly A, Van 't Hof RJ et al: Moderate exercise protects against joint disease in a murine model of osteoarthritis. Front Physiol. 2022;13:1065278.
34. Griffin TM, Huebner JL, Kraus VB, Yan Z, Guilak F. Induction of osteoarthritis and metabolic inflammation by a very high-fat diet in mice: effects of short-term exercise. Arthritis Rheum. 2012;64(2):443–53.
35. Hahn AK, Batushansky A, Rawle RA, Prado Lopes EB, June RK, Griffin TM. Effects of long-term exercise and a high-fat diet on synovial fluid metabolomics and joint structural phenotypes in mice: an integrated network analysis. Osteoarthritis Cartilage. 2021;29(11):1549–63.
36. van Osch GJ, van der Kraan PM, Vitters EL, Blankevoort L, van den Berg WB. Induction of osteoarthritis by intra-articular injection of collagenase in mice. Strain and sex related differences. Osteoarthritis Cartilage. 1993;1(3):171–7.
37. Mausset-Bonnefont AL, Cren M, Vicente R, Quentin J, Jorgensen C, Apparailly F, Louis-Plence P. Arthritis sensory and motor scale: predicting functional deficits from the clinical score in collagen-induced arthritis. Arthritis Res Ther. 2019;21(1):264.
38. Ter Heegde F, Luiz AP, Santana-Varela S, Magnusdottir R, Hopkinson M, Chang Y, Poulet B, Fowkes RC, Wood JN, Chenu C. Osteoarthritis-related nociceptive behaviour following mechanical joint loading correlates with cartilage damage. Osteoarthritis Cartilage. 2020;28(3):383–95.

Publisher's Note